THE JOURNAL OF PHYSICAL CHEMISTRY B

Article

Cite This: J. Phys. Chem. B 2018, 122, 4101−4114

pubs.acs.org/JPCB

Ab Initio Force Fields for Organic Anions: Properties of [BMIM][TFSI], [BMIM][FSI], and [BMIM][OTf] Ionic Liquids

Jesse G. McDaniel,† Chang Yun Son, and Arun Yethiraj*

Department of Chemistry, University of Wisconsin, 1101 University Avenue, Madison, Wisconsin 53706, United States

Supporting Information

ABSTRACT: Room-temperature ionic liquids (ILs) composed of organic anions bis(trifluoromethanesulfonyl)imide (TFSI), bis(fluorosulfonyl)imide (FSI), and trifluoromethanesulfonate (OTf) exhibit interesting physical properties and are important for many electrochemical applications. TFSI and FSI form "hydrophobic" ILs, immiscible with water but miscible with many organic solvents and polymers; for computer simulation studies, it is thus essential to develop force fields for these anions that are transferable among this wide variety of chemical environments. In this work, we develop entirely ab initio force fields for the TFSI, FSI, and OTf anions and predict the properties of corresponding 1-butyl-3-methylimidazolium ILs. We discuss important subtleties in the force field development related to accurately modeling conformational flexibility, that is, relaxed torsional profiles and intramolecular electrostatic interactions. The TFSI anions have notable conformational flexibility in the IL, and we predict approximately 70% cisoid and 20% transoid conformations, which is largely driven by cation/anion ion-pair interactions and is opposite to the trend expected from the anion ab initio potential energy surface. The favorable interactions between the cation and cisoid TFSI conformations result in a shoulder in the cation/anion radial distribution function at short distances, whereas interconversion between cisoid and transoid conformations occurs on a commensurate time scale as ion diffusion processes. In addition to this physical insight on anion effects, we expect that these force fields will have important applications for studying a variety of complex electrolyte systems.

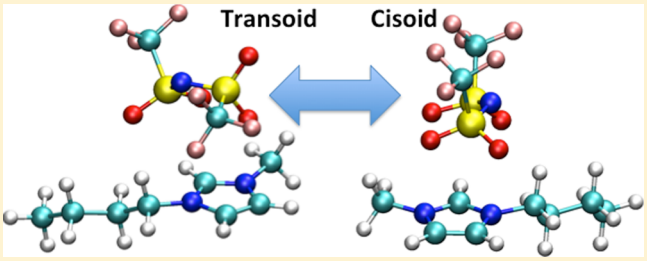

1. INTRODUCTION

Bis(trifluoromethanesulfonyl)imide (TFSI) anions constitute some of the most practically important and well-studied room-temperature ionic liquids (ILs) to date.[1] ILs composed of TFSI anions and imidazolium-based cations such as 1-butyl-3-methylimidazolium (BMIM) exhibit lower viscosity and higher conductivity than other ILs, making them well-suited for use in electrolytes or extracting solvents. In addition, [BMIM][TFSI] is immiscible with water, leading it to be termed a "hydrophobic" IL and demonstrating the interesting result that "ionic" does not necessarily imply hydrophilic.[2] The TFSI anion exhibits particular structural characteristics that imbue the resulting IL with its interesting properties. For example, the anion has significant conformational freedom because of its flexible S−N−S bonds, which has an important effect on lowering both the melting point and viscosity.[3] The electron-withdrawing CF_3SO_2 groups result in a large electrochemical stability window that makes [BMIM][TFSI] well-suited for electrochemical applications.[2] Altering these electron-withdrawing groups by forming the similar bis(fluorosulfonyl)imide (FSI) anion modulates the electrochemical stability, which can be utilized in electrochemical applications to form solid−electrolyte interface passivating layers.[4]

The TFSI anion is also an important component of many electrolytes for next-generation lithium batteries. Higher-energy-density anodes (lithium metal) and cathodes (lithium−sulfur) exhibit stability problems that can be reduced by employing solid-state or polymer−gel electrolytes. For such Li/polymer electrolytes, TFSI often serves as an optimal counterion because of the low lattice energy of LiTFSI salt and high miscibility of TFSI with organic solvents and polymers.[5−9] These applications have prompted structural studies of TFSI-based alkali metal salts as pure crystals, in polymer mixtures, and in organic solvents. X-ray diffraction, infrared and Raman spectroscopy, and ab initio techniques have found that TFSI anions exist in two distinct conformational motifs in the condensed phase, depending on the nature of complexing cation, phase, and solvent.[10−16] For example, in LiTFSI crystals, the anion exhibits a transoid conformation with C_2 symmetry,[10] 1,3-dimethylimidazolium (DMIM)/TFSI crystal structures comprise cisoid TFSI configurations,[17] and Li/polymers, Li electrolytes, or room-temperature ILs contain populations of both transoid and cisoid TFSI configurations with the relative fraction sensitively dependent on both system and temperature.[11−15] These interesting observations indicate that anion conformational flexibility is an important property of TFSI as a constituent of ionic condensed-phase systems.

Received: February 3, 2018
Revised: March 12, 2018
Published: March 14, 2018

DOI: 10.1021/acs.jpcb.8b01221
J. Phys. Chem. B 2018, 122, 4101−4114

Computer simulations are a powerful tool for investigating the properties of such complex electrolytes and IL systems.[18,19] For ionic systems containing TFSI anions, simulations may provide important insight into the physics dictating the fraction of cisoid/transoid anion conformations and the subsequent effect on other condensed-phase properties. A correct physical description and interpretation requires force fields that accurately capture the balance of intra and intermolecular energetics of the different TFSI conformers. Because of the variety of applications of TFSI anions, transferability of these force fields is extremely important if the models are to be applied to study neat ILs, IL mixtures, or electrolytes containing aqueous, organic, or inorganic constituent species. Furthermore, related anions such as FSI are also important electrolyte components, and thus, it is desirable that force field parameters are transferable to these related species. To achieve these transferability demands, it is essential that force fields contain the correct balance of physical interactions, such as electrostatics, polarization, and dispersion, correctly partitioned among atom types.

For a comprehensive synopsis of IL force field development and simulations of these and related systems, we defer to prior review articles[20,21] and a recent article by McDaniel et al.[22] We additionally note the recent work by Uhlig et al.[23] detailing a methodology for ab initio development of coarse-grained IL force fields, and also, previous simulation studies and force field development specifically focused on [BMIM][TFSI] and related ILs.[24−32] Rather than discussing all related prior work, we focus on the very pertinent work of Borodin and coworkers,[28] which comprehensively discusses the conformational and dynamic properties of TFSI- and FSI-based ILs predicted using accurate, polarizable force fields,[26,27,33−36] with comparisons against pulsed-field gradient NMR experiments. Notable findings were the prevalence of both cisoid and transoid anion conformations and the correlation of conformational interconversion with ion diffusion rates. Throughout this manuscript, we attempt to illuminate both similarities and differences of our predictions with those of Borodin et al.,[28] which we believe to be essential for correctly interpreting the complex physics in these systems. As our present work and Borodin's work[28] both utilize relatively sophisticated, polarizable force fields constructed from detailed ab initio parametrization, the fact that discrepancies exist suggests the need for extreme care in the development of IL force fields, whereas the approach of ad hoc empirical parametrization should be discouraged.

In this work, we provide a systematic methodological description for the development of an entirely ab initio and transferable force field for TFSI and related FSI and trifluoromethanesulfonate (OTf) anions. Because of the observed importance of conformational flexibility, we present a detailed discussion of the ab initio conformational potential energy surfaces (PESs) and best practices for accurately capturing these energetics in the anion force field. We find that typical ad hoc methods of scaling 1−4 intramolecular nonbonded terms are not appropriate for these anions, as they introduce artificial cut offs to the very large intramolecular electrostatic interactions. We describe how nonbonded force field parameters can be developed based on previously reported approaches[22,37,38] utilizing symmetry-adapted perturbation theory (SAPT)[39−41] but in this case utilizing small "probe" molecules to reduce the computational expense of requisite electronic structure calculations for these relatively large anions. We show that this parametrization scheme introduces no inherent bias for a particular interaction type, and intermolecular interactions between anion/anion, anion/cation, and anion/neutral dimer species are described with equally high fidelity utilizing a single set of parameters and combination rules. With the exception of atomic charges and equilibrium bond and angle values, all anions utilize the same force field parameters for similar atom types, demonstrating the transferability of the parameterization.

We apply these ab initio anion force fields to study the ILs [BMIM][TFSI], [BMIM][FSI], and [BMIM][OTf]. We find that the predicted densities, heats of vaporization, diffusion coefficients, and conductivities are in excellent agreement with the corresponding experimental data. From our simulations, we present a detailed analysis of the cisoid/transoid TFSI conformations in [BMIM][TFSI] and the corresponding influence on the bulk IL properties. We demonstrate that cisoid TFSI conformations are energetically stabilized by cation/anion intermolecular interactions, which more than counterbalances the higher cisoid torsional energy of the anion ab initio PES. This results in a ∼70 and 20% cisoid and transoid population in [BMIM][TFSI] and indicates that ion-pair interactions in ILs may generally dictate TFSI condensed-phase conformations. We predict a close-contact shoulder in the cation/anion pairwise radial distribution function that is attributed entirely to the TFSI cisoid configuration. By conducting additional conformer-biased simulations, we find that interconversion between cisoid and transoid TFSI conformers is coupled to ion mobility, enhancing diffusion in [BMIM][TFSI] by 20−30%. We believe that our present force fields are uniquely suited for modeling the wide range of electrolyte and ionic systems comprising TFSI and related anions because of their exceptional transferability and physically motivated parametrization. In addition, our present work is novel in that it constitutes an entirely ab initio prediction of the liquid-state properties of [BMIM][TFSI], [BMIM][FSI], and [BMIM][OTf] ILs.

2. METHODS

2.1. Nonbonded Force Field Parametrization. We parametrize nonbonded force field components for TFSI, FSI, and OTf anions based on the framework of SAPT.[39−41] We briefly describe the essential details of this approach, whereas a more comprehensive discussion may be found in the previous work of McDaniel and Schmidt.[37,38] The force field is parametrized to exhibit a one-to-one correspondence with the energy decomposition given by SAPT; namely explicit terms exist for exchange−repulsion, electrostatic, induction, dispersion, and higher-order (delta Hartree−Fock) interactions. Furthermore, each energy term is decomposed into short-range and long-range components, where the long-range components correspond to analytic asymptotic expressions based on multipole expansions of Rayleigh−Schrodinger perturbation interactions and the short-range terms account for charge-overlap corrections to these energies.[38] Force field parameters describing the asymptotic interactions such as charges, polarizabilities, and dispersion coefficients are explicitly fit to monomer properties, specifically the electron density and static- and frequency-dependent density susceptibilities.[37] The short-range force field terms are modeled by Born−Mayer exponential functions, with the parameters explicitly fit to the residual of SAPT interaction energy calculations and the asymptotic energy contributions. The functional form and all force field parameters developed in this work are given in the

DOI: 10.1021/acs.jpcb.8b01221
J. Phys. Chem. B 2018, 122, 4101−4114

Supporting Information. Importantly, our force field is compatible with and easily implemented in standard molecular dynamics (MD) software packages including GROMACS,[42] LAMMPS,[43] and OpenMM.[44]

We develop a single set of nonbonded force field parameters for the five elements (C, N, O, S, and F) comprising the three anions, TFSI, FSI, and OTf, the chemical structures of which are shown in Figure 1. We find that this is possible for all parameters except the partial atomic charges, which must be fit specifically for each anion.

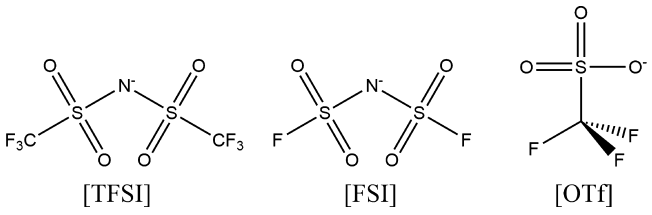

Figure 1. Anions TFSI, FSI, and OTf.

The parameterization of TFSI requires special consideration because of its conformational flexibility and size, the latter making electronic structure calculations computationally intensive. To examine the conformational freedom, we compute the PES of TFSI as a function of two of its $\theta_{O-S-N-S}$ dihedral angles, which provide the primary flexibility of the anion. The TFSI PES is shown in Figure 2, as computed at the PBE0/AVTZ level of theory, with all other degrees of freedom (bonds, angles, etc.) relaxed at every point on the surface (vide infra). The two important transoid and cisoid conformations are denoted as "a" and "b", respectively. We find that the transoid conformation is the global minima, ~5 kJ/mol lower in energy than cisoid (and a similar barrier height), and thus, interconversion between these conformations should be thermally facile. Two other conformations "c" and "d" on the PES are illustrated for comparison; conformation "c" is the most symmetric (C_{2v}) conformation of the anion but is ~14 kJ/mol higher in energy than the transoid conformation because of the steric repulsion of the $-CF_3$ groups. The most unfavorable conformations of the anion correspond to "d"-like structures, in which the $-CF_3$ groups exhibit extreme steric repulsion and the θ_{S-N-S} angle is significantly distorted as a result. Our results for the TFSI conformational energetics are in semiquantitative agreement with previous ab initio studies;[11−14,28] however, the delocalized charge of the anion makes the quantitative predictions particularly sensitive to the employed level of theory, that is, basis sets/electron correlation.

We expect that in the bulk IL, TFSI will exist in an ensemble of structures intermediate between the transoid "a", cisoid "b", and "c" motifs. We therefore consider the "a" and "c" TFSI structures in the parameterization of the nonbonded interactions. Previous works[22,37] utilized SAPT interaction energies between *homomolecular dimers* for force field parameterization; this is intractable for TFSI dimers because of the computational expense and large dimer conformational space. Instead, we take a different approach, employing small "probe" molecules to sample the orientation dependence of short-range intermolecular interactions with the target molecule (TFSI); this results in much greater computational efficiency, with additionally reduced dimensionality of the dimer configurational space. A key result of this work is that the specific choice of the probe molecule does not significantly bias the parameterization of the target molecule (TFSI); this finding is important for force field transferability and we believe is a result of the direct one-to-one correspondence between force field terms and the SAPT energy decomposition.

We calculate DFT−SAPT[45−48] interaction energies for dimers of TFSI and methane "probe" molecules, considering both the "a" and "c" TFSI geometries. Methane is chosen as a probe molecule because it is small and roughly spherical, and analogous SAPT-based force field parameters have been previously developed.[37,49] We generate several thousand configurations of TFSI/methane dimers randomly chosen to span the various dimer orientations and located at separations between 0.8 and 1.2 times the van der Waals contact surface; this large number of dimer configurations is considered only for completeness, and methods for intelligently choosing configurations may be employed when necessary.[50] All SAPT calculations are conducted using the MOLPRO software package,[51] with similar basis sets and asymptotic corrections as used previously.[37] The fits to the SAPT interaction energies for TFSI "a"/methane dimers are shown in Figure S1; these are the only SAPT calculations in this work that are used to fit nonbonded force field parameters, and all other SAPT calculations are for validation purposes rather than parametrization. For dimer configurations with total energies less than $\sim 5k_BT$, the root-mean-square (rms) error of the force field fit is ~2 kJ/mol, with the error dominated mostly by repulsive configurations; this error is intrinsically due to limitations imposed by the approximate force field functional form and is not specific to the parameterization approach.[37] In Figure S2,

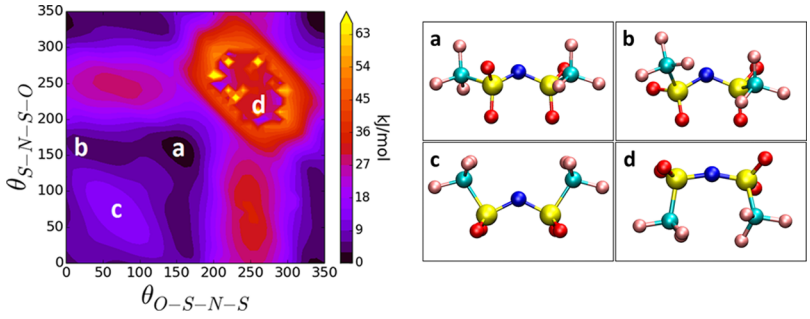

Figure 2. TFSI dihedral PES computed at the PBE0/AVTZ level of theory with all remaining degrees of freedom fully relaxed at each point on the surface. The PES is a function of two of the O−S−N−S dihedral angles that constitute the main conformational flexibility of the anion. Snapshots of the transoid "a" and cisoid "b" TFSI geometries and additional conformations "c" and "d" are shown and their respective location on the PES is labeled.

DOI: 10.1021/acs.jpcb.8b01221
J. Phys. Chem. B 2018, 122, 4101−4114

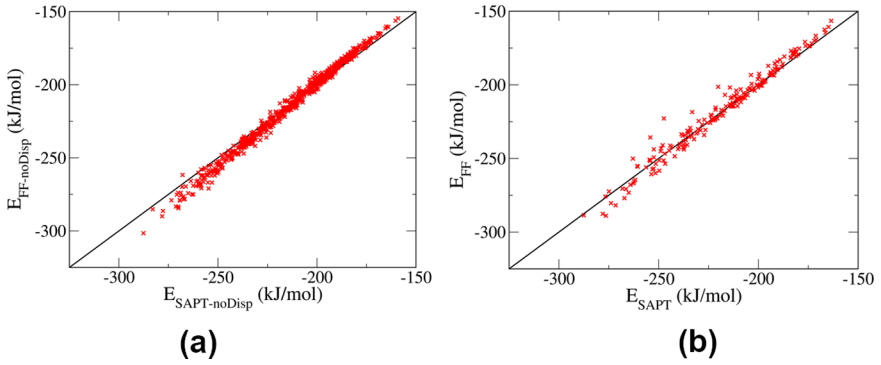

Figure 3. Comparison of force field interaction energies (E_{FF}) and SAPT interaction energies (E_{SAPT}) for dimer configurations of (a) TFSI/imidazolium and (b) OTf/EMIM. Each point on the graph corresponds to a specific dimer configuration, and the $y = x$ line is shown to guide the eye. Because of the computational expense, the TFSI/imidazolium SAPT energies do not include dispersion contributions ($E_{SAPT-noDisp}$) and are compared to the dispersion-free force field energy ($E_{FF-noDisp}$).

we show similar comparisons between SAPT interaction energies and force field terms for TFSI "c"/methane dimers, modeled using the parameters developed from the TFSI "a"/methane dimer calculations. The rms error for these configurations is similarly ~2 kJ/mol, indicating that for the target force field accuracy, the nonbonded TFSI parameters can be decoupled from the TFSI conformational flexibility.

The TFSI parameters fit to methane "probe" dimer calculations are transferable to TFSI/BMIM interactions. We compute SAPT interaction energies between the TFSI anion and imidazolium cation for several hundred dimer configurations; these resemble the primary cation/anion attractive interactions in the [BMIM][TFSI] bulk IL. Because of the computational expense, we compute only exchange, electrostatic, and induction SAPT energies and neglect the expensive dispersion term; this is a sufficient test of parameter transferability as dispersion parameters are fit solely on the basis of monomer response calculations and not to SAPT interaction energies.[37] Comparisons of these SAPT energies to corresponding force field terms are shown in Figures S3 and S4 for TFSI geometries "a" and "c", respectively, and a comparison of the total interaction energy (excluding dispersion) for TFSI "a"/imidazolium dimers is shown in Figure 3a; the imidazolium parameters used to generate cross-terms are taken from our previous work.[22] From these comparisons, it is evident that the TFSI nonbonded parameters developed using methane "probe" molecule calculations are equally accurate for modeling the TFSI/imidazolium cation/anion interactions; the rms error of the force field for the dimer configurations of Figure 3a is ~3.5 kJ/mol, which is comparable to the accuracy of the TFSI/methane interactions, even though the cation/anion interactions are ~30 times larger in magnitude!

For the other anions, FSI and OTf, partial atomic charges are specifically fit for each anion and all other nonbonded force field parameters are taken to be the same as those for TFSI, determined as described above. To verify the transferability, we compute SAPT interaction energies for three sets of molecular ion dimers, namely, FSI/imidazolium, OTf/OTf, and OTf/1-ethyl-3-methylimidazolium (EMIM). Comparisons between SAPT interaction energies and force field components for these dimers are shown in Figures S5–S7, with rms errors for the force field total interaction energy of ~7, 4, and 4 kJ/mol, respectively; we note that the absolute rms error is strongly dependent on the van der Waals separation distances chosen to generate dimer configurations, with generally greater error for closer separations. The transferability of the force field parameterization is illustrated by the highly accurate description of the interaction energies for OTf/EMIM dimers shown in Figure 3b, as all parameters for OTf (except charges) are identical to those of the TFSI anion, developed on the basis of TFSI/methane dimer calculations.

2.2. Torsion Force Field Parametrization. The parameterization of the force field for torsional rotations has several subtleties that can have an impact on the quality and transferability of the overall force field. The torsional force field is usually the "leftover energy". One constructs an ensemble sampling the important torsion conformations of a molecule, computes an ab initio PES as a function of these conformational degrees of freedom, and fits the dihedral (torsion) potentials to the residual energy difference between the ab initio PES and all other force field terms. There are subtleties, however, in calculating and fitting the ab initio PES, which we now discuss.

In particular, it is important to consider *relaxed* dihedral surfaces, in which all other degrees of freedom are relaxed (minimized) at every conformation for *both* ab initio calculations *and* force field models. This is because the coupling between the angles (and potentially bond lengths) to the dihedral surface has very important consequences for force field fitting. For example, for the TFSI PES shown in Figure 2, the equilibrium θ_{N-S-C} and θ_{N-S-O} angles change by ~8° between transoid "a" and cisoid "b" conformations across the dihedral surface. Unless a force field is constructed such that equilibrium angle values are parametric on (coupled to) the dihedral surface, the relatively stiff harmonic angle potentials will impose significant energetic discrepancies in the PES fit.

We express the *relaxed* torsional energy as

$$E(\{\phi_i\})^{H^\alpha} = \min^{H^\alpha}_{\theta_i, r_i} E(\{\phi_i, \theta_i, r_i\}) \quad (1)$$

where H^α represents either the QM Hamiltonian (H^{QM}) used to compute the ab initio PES or the force field/molecular mechanics Hamiltonian (H^{MM}), $\{\phi_i,\theta_i,r_i\}$ is the set of all dihedrals (ϕ_i), angles (θ_i), and bonds (r_i) describing the conformation, and $\min^{H^\alpha}_{\theta_i,r_i}$ means minimizing the energy with respect to the bonds and angles according to the Hamiltonian, H^α. The dihedral potentials are then least-squares fit based on the energy difference between the QM- and MM-*relaxed* dihedral surfaces (for simplicity, we omit a weighting function, which may be important in certain cases)

DOI: 10.1021/acs.jpcb.8b01221
J. Phys. Chem. B 2018, 122, 4101–4114

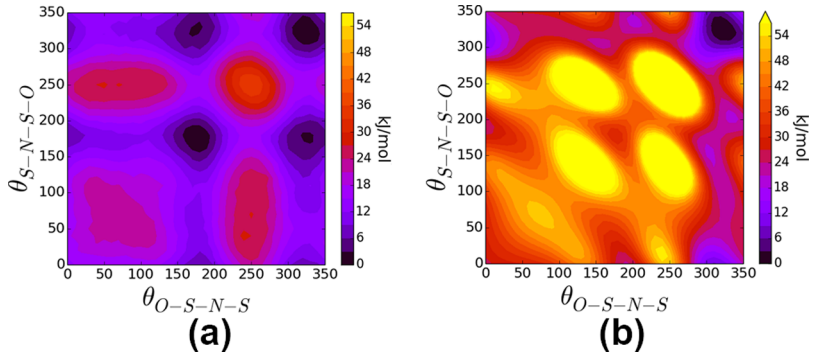

Figure 4. Ab initio PES for an FSI anion as a function of the two main dihedral angles. (a) "Relaxed" dihedral PES generated by relaxing all other degrees of freedom at each conformation and (b) rigid dihedral PES for which bonds and angles are fixed to their values at the global minima.

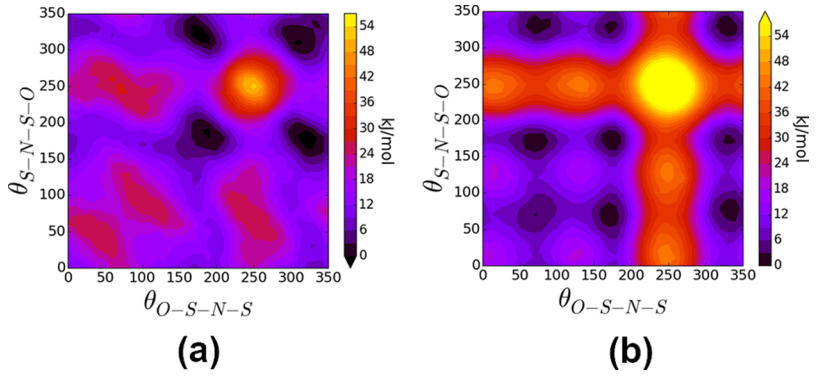

Figure 5. Force field-generated PES for an FSI anion as a function of the two main dihedral angles. (a) Fit to configurations (bonds, angles) of the QM-relaxed surface and (b) same potential but with geometries (bonds, angles) relaxed using the MM Hamiltonian.

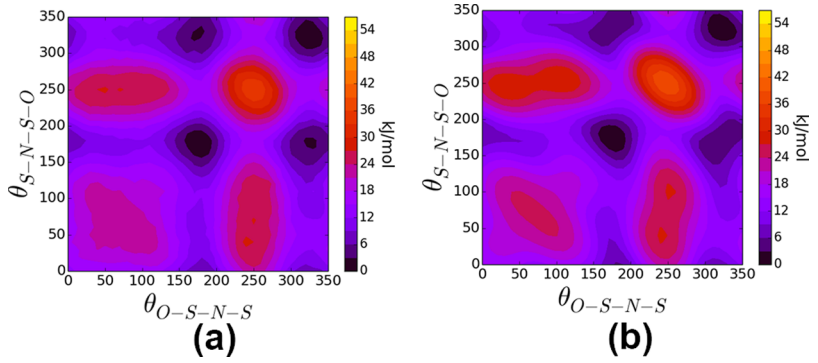

Figure 6. Relaxed PES for an FSI anion as a function of the two main dihedral angles. (a) MM surface and (b) QM surface. For each point on the surface, all other degrees of freedom have been relaxed according to the corresponding Hamiltonian.

$$\chi^2 = \sum_{\{\phi_i\}} (E(\{\phi_i\})^{H^{MM}} - E(\{\phi_i\})^{H^{QM}})^2 \quad (2)$$

We emphasize that the QM- and MM-relaxed surfaces have different bond and angle values for each dihedral conformation. We consider the dihedral PES of the FSI anion to illustrate the necessity of employing the relaxed dihedral surfaces rather than rigid dihedral surfaces for fitting. Figure 4 compares the ab initio, relaxed dihedral PES for FSI (Figure 4a) to a "rigid" dihedral PES for FSI in which the bonds and angles have been fixed to their equilibrium values at the global minima (Figure 4b). It is clear that the relaxed dihedral surface is much smoother than the rigid dihedral surface, and relaxing the bonds and angles at each conformation reveals several additional local minima that were obscured in the rigid dihedral scan. Henceforth, we will thus only consider relaxed ab initio dihedral PESs such as that shown in Figure 4a for the FSI anion.

It is important to generate the MM-relaxed surface rather than directly employing the conformations of the QM-relaxed surface because the coupling between the equilibrium bond and angle values across the dihedral surface is absent in the force field functional form. In Figure 5a, we show the MM PES generated by directly fitting the QM-relaxed dihedral surface using the corresponding QM conformations. The resulting MM PES appears qualitatively similar to the ab initio PES (Figure 4a) but exhibits significant skew or stretching of the local minima and dihedral barriers because of the inherent coupling with equilibrium bond and angle values. However, Figure 5a is a misleading representation of the conformational freedom

DOI: 10.1021/acs.jpcb.8b01221
J. Phys. Chem. B 2018, 122, 4101−4114

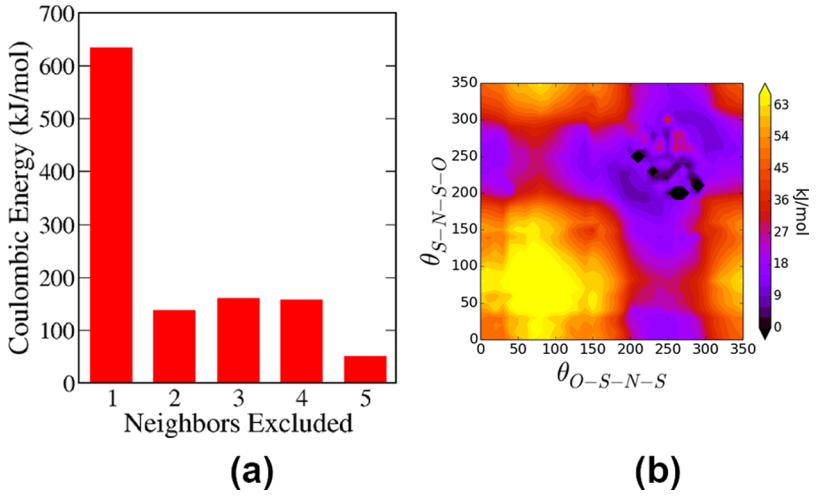

Figure 7. (a) Intramolecular Coulombic energy of a TFSI anion as a function of exclusions based on bond topology; 1 denotes exclusions of nearest neighbors, 2 is exclusions of nearest and next-nearest neighbors, etc. (b) Coulombic energy surface for TFSI as a function of dihedral angles, computed by including intramolecular Coulomb interactions only for 1−5 atompairs and greater.

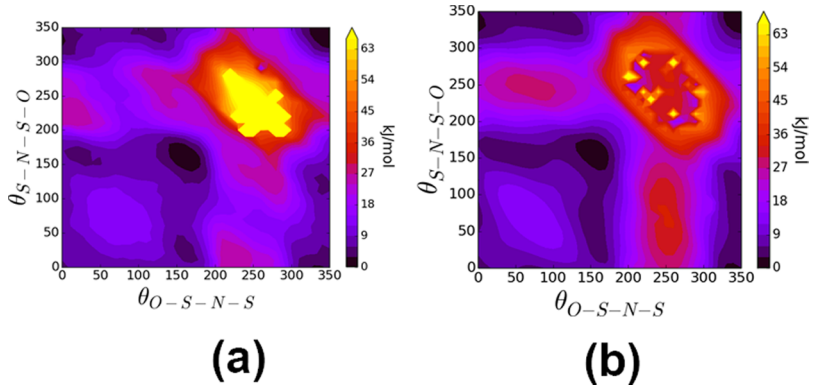

Figure 8. Relaxed PES for a TFSI anion as a function of the two main dihedral angles. (a) MM surface and (b) QM surface. For each point on the surface, all other degrees of freedom have been relaxed according to the corresponding Hamiltonian.

determined by the force field Hamiltonian because the PES is a function of the relaxed QM bonds and angles that are not consistent with the MM bonds and angles over the entire surface. Using the same MM Hamiltonian to generate the MM-relaxed dihedral surface results in the PES shown in Figure 5b; this is the appropriate dihedral surface that reflects the torsional freedom of the MM Hamiltonian. Clearly, the MM dihedral surface (Figure 5b) exhibits significant deviations from the QM dihedral surface (Figure 4a) due to the fact that the relaxed MM conformations were not used for fitting (eq 2) and the force field cannot adequately describe the bond, angle, and dihedral coupling.

When the prescribed procedure is followed (eq 2), the relaxed MM dihedral surface is very similar to the relaxed QM dihedral surface, as shown in Figure 6. It is evident that the relaxed MM dihedral surface (Figure 6a) closely approximates the relaxed QM dihedral surface (Figure 6b) and should therefore provide an accurate description of the conformational distribution.

The parameterization of the TFSI anion is more complex because of the additional steric interaction imposed by the $-CF_3$ groups. The incorporation of steric repulsion into dihedral potentials is a subtle component of force fields, and there is no generally accepted procedure. A consequence is that there are different recipes for treating the intramolecular nonbonded interactions between sites separated by three bonds (1−4 interactions). These interactions are either omitted, included fully, included only for specific pairs, or included but scaled by a factor such as 0.5 or 0.83.[52−55] The reason for these discrepancies is that force fields employ functional forms that are appropriate at long separations but not at the short separations relevant for intramolecular interactions. The fact that these interactions cannot be ignored, however, creates a general dilemma for force field development.

The case of the TFSI anion illustrates several issues of general concern. In TFSI, the atomic partial charges are large, for example, ∼+0.8 on sulfur and ∼−0.5 on oxygen (Supporting Information). Coulombic 1−4 interactions between the force field Drude oscillators and these large partial charges can lead to overpolarization problems;[56] indeed, we find that with Coulombic 1−4 interactions, Drude oscillator displacements can be several tenths of an angstrom for various conformations of the dihedral surface, suggesting that it may be preferable to exclude such interactions. Additional problems with including intramolecular Coulombic interactions result from the fact that choosing an arbitrary bond-separation cut off necessarily creates charged ionic subgroups within the molecule that causes large oscillations in the intramolecular energy. This is shown in Figure 7a, which plots the intramolecular Coulombic energy for the TFSI anion (averaged over the

DOI: 10.1021/acs.jpcb.8b01221
J. Phys. Chem. B 2018, 122, 4101−4114

Table 1. Bulk Properties for [BMIM][TFSI] at 300 K[a]

	ρ (kg/m^3)	ΔH_{vap} (kJ/mol)	$E_{coh.}$ (kJ/mol)	D_+ (10^{-5} cm^2/s)	D_- (10^{-5} cm^2/s)	σ (S/m)
MD	1405	115(5)	−468	0.020(5)	0.017(5)	0.3(1)
Exp.[3,63−65]	1438	130(5)	N/A	0.03(1)	0.03(2)	0.39(5)

[a]Listed in parenthesis are the uncertainties of the last reported digit. The extensive energetic quantities are per ion pair.

Table 2. Bulk Properties for [BMIM][FSI] at 300 K[a]

	ρ (kg/m^3)	ΔH_{vap} (kJ/mol)	$E_{coh.}$ (kJ/mol)	D_+ (10^{-5} cm^2/s)	D_- (10^{-5} cm^2/s)	σ (S/m)
MD	1321	132(5)	−462	0.016(5)	0.013(5)	0.3(1)
Exp.[66]	1355		N/A			0.85

[a]Listed in parenthesis are the uncertainties of the last reported digit. The extensive energetic quantities are per ion pair.

Table 3. Bulk Properties for [BMIM][OTf] at 300 K[a]

	ρ (kg/m^3)	ΔH_{vap} (kJ/mol)	$E_{coh.}$ (kJ/mol)	D_+ (10^{-5} cm^2/s)	D_- (10^{-5} cm^2/s)	σ (S/m)
MD	1252	121(5)	−462	0.022(5)	0.013(5)	0.3(1)
Exp.[3,63]	1300		N/A	0.02(1)	0.015(5)	0.37(5)

[a]Listed in parenthesis are the uncertainties of the last reported digit. The extensive energetic quantities are per ion pair.

dihedral surface, Figure 2) as a function of the neighbors excluded, that is, excluding 1−4 interactions is equivalent to excluding through the third neighbor. Unfortunately, there is no systematic monotonic trend with excluded neighbors, and the intramolecular Coulomb energy fluctuates as a function of neighbors excluded. For example, the 1−4 Coulomb interaction between sulfur and oxygen atoms is a large attractive interaction (based on the partial charges), and thus, excluding 1−4 interactions leads to an *increase* in the intramolecular Coulomb repulsion by ∼20%.

The unphysical fluctuations in the force field intramolecular Coulomb energy as a function of exclusions indicate that this term may hinder an accurate description of the dihedral PES. We explore this further by computing the intramolecular Coulomb energy for TFSI as a function of dihedral conformations for a fixed choice of exclusions, namely, excluding 1−4 interactions but including 1−5 pairs and beyond. This Coulomb energy surface is shown in Figure 7b; comparison with the ab initio dihedral PES of TFSI (Figures 2 and 8b) indicates that there is no positive correlation between these surfaces, and in fact, they are somewhat anticorrelated. This suggests that the incorporation of intramolecular Coulomb interactions in the force field will hinder rather than benefit the accurate description of the dihedral PES for TFSI.

On the basis of this analysis, we fit the TFSI dihedral PES using the following approach. All intramolecular Coulombic interactions involving static charges are excluded, and the remaining intramolecular nonbonded interactions (exchange−repulsion, van der Waals, etc.) are included only for 1−5 interactions and beyond, capturing steric interactions involving the $-CF_3$ groups; we note that all intramolecular polarization interactions are incorporated using screened Thole functions, see Supporting Information. The dihedral potentials are then fit to the residual energy differences between the relaxed QM and MM surfaces. The resulting relaxed MM dihedral surface is shown in Figure 8a and compared with the relaxed QM surface in Figure 8b. The MM dihedral surface accurately reproduces the essential important features of the QM surface, including the important transoid and cisoid minima "a" and "b" and the relative steric energy penalties for conformations "c" and "d" (Figure 2). Although our procedure for fitting the dihedral surface may be specific to smaller anions (intramolecular Coulomb interactions cannot be fully excluded for arbitrary-sized molecules/polymers), our analysis of the importance of fitting relaxed surfaces and the problematic intramolecular Coulomb energetic contribution has general relevance. We note that although TFSI force fields have previously been developed based on ab initio dihedral PESs,[24,26,29,31] none of these works present an explicit comparison between the relaxed MM and relaxed QM dihedral surfaces, making it difficult to evaluate the relaxed torsion profiles of these MM models.

3. RESULTS

3.1. Bulk Liquid Properties. We use MD simulations to predict the bulk liquid properties of [BMIM][TFSI], [BMIM][FSI], and [BMIM][OTf] at 300 K, 1 bar, using the force fields for anions developed in this work. For the BMIM cation, we employ the force field developed in our previous work,[22] with cross-interactions given by simple combination rules (Supporting Information). After equilibration, statistics are collected from 50 ns trajectories to obtain converged dynamic properties.[22] To access these time scales, we utilize the OpenMM software implemented on graphics processing units,[44] employing an efficient dual thermostat (1 ps^{-1} friction coefficients), and extended Lagrangian algorithm[57] for polarization.

The dual thermostat scheme typically requires ∼1 ps^{-1} friction coefficients to ensure equipartition and correct for temperature exchange between hot and cold degrees of freedom; consequently, there will be deviation from the true Hamiltonian dynamics.[58] We propose a correction based on shorter simulations utilizing a fully self-consistent field treatment of polarization, for which weaker-coupling thermostats may be used as there is no cold heat sink. We conduct ∼10 ns simulations of this type with the GROMACs software[42] using a Nose−Hoover thermostat, which insignificantly perturbs the dynamics.[58] From these simulations, we estimate the diffusion coefficients (and similarly conductivities) by

$$D = D^{\text{Langevin}}(50\text{ ns})\frac{D^{\text{SCF}}(10\text{ ns})}{D^{\text{Langevin}}(10\text{ ns})} \quad (3)$$

The bulk properties for [BMIM][TFSI], [BMIM][FSI], and [BMIM][OTf] obtained from simulations are given in Tables

DOI: 10.1021/acs.jpcb.8b01221
J. Phys. Chem. B 2018, 122, 4101−4114

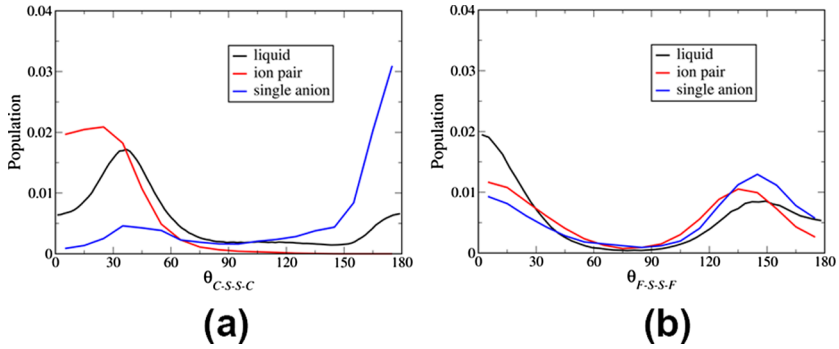

Figure 9. Pseudodihedral distribution of (a) TFSI and (b) FSI anions in the liquid phase, as single ion pairs with BMIM cations, and as isolated anions. Cisoid conformations correspond to ~0 < θ < 60 and transoid conformations correspond to ~120 < θ < 180.

1−3 and compared with available experimental data. All predicted properties are in semiquantitative agreement with experiment, with predicted densities (ρ) generally ~2−3% too low (vide infra). The predicted dynamic properties including the cation (D_+) and anion (D_-) diffusion coefficients and IL conductivity (σ) are mostly within experimental uncertainty; for [BMIM][FSI], the predicted conductivity is somewhat too low, with the source of this discrepancy unclear considering the good agreement for the other systems. We have omitted finite-size corrections for the dynamic properties,[59] as these corrections are smaller than the statistical uncertainties reported in Tables 1−3; the relatively large statistical uncertainties of dynamic properties for ILs have been discussed elsewhere.[22] We note that the IL conductivities are ~20−40% lower than would be predicted assuming ideal behavior (Nernst−Einstein)[3] because of the collective, correlated motion among cations and anions.[60,61]

The enthalpy of vaporization (ΔH_{vap}) of [BMIM][TFSI] is predicted ~10% too low compared to experiment, with this error at least partially due to the approximation of only single ion pairs in the gas phase.[22] Furthermore, we provide predictions of the IL cohesive energy ($E_{coh.}$), which is important for the physical interpretation of other liquid properties[22] but very difficult to obtain experimentally.[62] Interestingly, we find that the cohesive energies for the three different ILs are all within ~1−2%, despite the different nature of the anions! This is contrasted with the heats of vaporization which are up to ~10% different between ILs, indicating that gas-phase ion-pair energies are more sensitive to the ion type than are the liquid cohesive energies.

Although the predicted IL densities are ~2−3% too low compared to experiment, this does not impact the prediction of other thermodynamic properties. This is because the predicted densities from a simulation are very insensitive to the force field parameters that govern the strength of intermolecular interactions, a consequence of the extremely large cohesive energies (~−450 kJ/mol per ion pair). For example, altering the force field to reduce the electrostatic cohesive energy by >100 kJ/mol per ion pair only results in a ~3% density change for the IL [BMIM][BF4]![67] This is in stark contrast to much more weakly interacting organic solvents, for which relatively small changes in the intermolecular interactions (e.g., non-additive dispersion effects) significantly alter the prediction of liquid densities.[49] Thus, unlike for common organic liquids,[53] the predicted density of ILs should not be used as a benchmark for the nonbonded force field parameters because of the strong insensitivity.

The density of ILs is instead largely dictated by optimal ion packing and is therefore sensitive to the molecular ion size and shape, that is, force field parameters such as equilibrium bond lengths, angles, and the dihedral PESs. Ion packing largely dictates many of the IL thermodynamic properties, as ILs composed of smaller and more symmetric molecular ions generally tend to have higher melting points; for example, tetramethylammonium- or DMIM-based ILs are often crystalline at room temperature. The IL density is very sensitive to ion size; to illustrate this point, we conduct additional simulations in which all bonds of the molecular ions were reduced in length by 2%. These reduced bond length simulations of [BMIM][TFSI] give a density that is ~4% higher than the original simulations. This sensitivity to molecular ion bond length implies that the exact ab initio prediction of IL density is difficult; for molecular anions, electronic structure calculations of bond lengths can vary by at least several percent for "reasonable" choices of theory and basis set.

The other thermodynamic properties, however, are not very sensitive to the exact ion size/bond lengths. Comparing the [BMIM][TFSI] simulations of different bond lengths, we find differences in the liquid cohesive energy of only ~1%, and we find no statistically significant differences between the mean square displacement of the ions or radial distribution functions (RDFs) between cation and anion atom pairs from the two different simulations. It is important to note that these comparisons are made using NPT simulations, which is the appropriate ensemble so that the system volume can relax to accommodate the slightly changing ion sizes. Our findings indicate that besides the prediction of density, the exact molecular ion bond lengths do not significantly affect the predictions of other liquid-state properties as long as simulations are run in the NPT ensemble (or NVT at the appropriately equilibrated density for the model). Because of the sensitivity of the predicted density to the molecular ion sizes and bond lengths and the difficulty in exactly determining these quantities from the electronic structure, we suggest that slightly scaling bond lengths to match experimental liquid densities would be the most physically justified empirical modification to an ab initio IL force field.

3.2. Influence of TFSI Cisoid and Transoid Distribution on [BMIM][TFSI] Bulk Properties. The most interesting structure/property relationship in [BMIM][TFSI] IL is the influence of the conformational flexibility of the TFSI anion on the ion packing, ion interaction strength, and resulting static and dynamic liquid properties. We find that the conformational population of TFSI is very different in the IL, when compared to the gas phase, whereas in contrast, the conformations of FSI

DOI: 10.1021/acs.jpcb.8b01221
J. Phys. Chem. B 2018, 122, 4101−4114

are similar in the IL and the gas phase. There are several distinct anion conformations that are potentially important constituents of the bulk [BMIM][TFSI] IL, most notably, the cisoid and transoid conformations. For both the TFSI and FSI anions, cisoid and transoid conformations can be identified by the "pseudo" dihedral angle, either $\theta_{C-S-S-C}$ or $\theta_{F-S-S-F}$ for the two different anions, respectively. In Figure 9, we plot the distribution of these dihedral angles for both anions in their respective ILs, [BMIM][TFSI] and [BMIM][FSI]. To elucidate the physics dictating the dihedral distibutions, we compute the analogous dihedral distributions for gas-phase ion pairs (BMIM/TFSI, BMIM/FSI) and gas-phase isolated anions (TFSI, FSI). Analyzing the FSI conformations first (Figure 9b), it is evident that there are approximately equal populations of cisoid and transoid conformers and the distribution is only moderately affected by the chemical environment. Thus, the FSI conformer distribution is largely determined by the energetics of the FSI torsional PES (Figure 6), which exhibits nearly isoenergetic minima for cisoid and transoid conformations. Such a result is expected when intra and intermolecular degrees of freedom are energetically uncoupled, and analogous conclusions for FSI conformations in similar ILs have been reported previously by Borodin et al.[28]

The dependence of TFSI conformation on chemical environment is much more interesting, as suggested by the numerous previous reports of variation of the TFSI conformer population among different ionic systems.[10−16] As shown in Figure 9a, there is a major shift in the distribution from transoid to cisoid conformations when TFSI anions are in the presence of BMIM cations. The net fraction of cisoid and transoid conformers is determined by integrating the dihedral distribution (Figure 9a) over appropriate partitions; we choose $0 < \theta < 60$ and $120 < \theta < 180$ to correspond to cisoid and transoid conformations, respectively. The result of this partitioning is shown in Figure 10. For isolated TFSI anions,

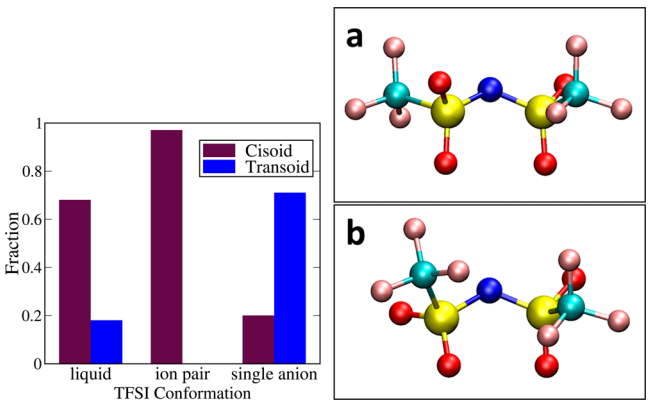

Figure 10. Fraction of transoid "a" and cisoid "b" TFSI conformers in different environments; liquid [BMIM][TFSI], gas-phase BMIM/TFSI ion pairs, and a single isolated TFSI anion.

the cisoid/transoid population is ∼20/70% with a greater fraction of transoid. In a two-state approximation, this corresponds to a relative energy stabilization of $\sim 1.5 k_B T$ for the transoid conformation, which is in good agreement with the TFSI torsional PES (Figure 8) and with previous studies.[11−14,28] Interestingly, in the [BMIM][TFSI] liquid, the TFSI conformer distribution is significantly different, with cisoid conformations more probable by an almost exactly inverted ratio of ∼70/20%! This conformational distribution leads to significantly different ion structuring in the liquid than would otherwise occur with a mostly transoid distribution.

In the gas phase, BMIM/TFSI ion pairs are composed entirely of cisoid TFSI conformers! This is because there are no steric or packing constraints in the gas phase, and the ion pair configuration is determined based solely on optimizing the intra and intermolecular interactions of the two ions. This clearly indicates that the ion-pair attraction of BMIM/TFSI is significantly more stable for cisoid TFSI conformers, and the resulting dihedral distribution is primarily due to *inter* rather than *intra*molecular energetics; thus, rationalizing liquid-phase conformer distributions solely based on the anion torsional energy[12] is inappropriate. We note that our results for TFSI ILs differ somewhat compared to the predictions of Borodin et al.,[28] who found identical TFSI conformer distribution in ILs as for gas-phase anions; the source of this deviation is unclear, potentially a subtle parametrization difference or equipartition effect. Additionally, these authors predicted nearly 50/50% transoid/cisoid fraction in a similar EMIM/TFSI IL, which is in better agreement with the analysis of experimental Raman measurements.[12] However, our conclusion of significant fraction of both conformers in the IL is consistent with both studies.

The structural properties of the IL are influenced by the TFSI conformations. In particular, a shoulder appears in the anion/cation pair distribution function (RDF) that can be attributed to the cisoid conformations. To address the impact of anion conformation on the liquid structure, we perform "biased simulations" employing artificial TFSI dihedral surfaces that impose an energetic penalty to bias the anion to either transoid or cisoid conformations; the explicit dihedral surfaces that we use in these simulations are given in the Supporting Information. To distinguish between the original (unbiased) and biased simulations, we use the following notation: the original simulation employing the ab initio TFSI dihedral surface is termed "TFSI-flexible"; the simulation employing the *biased transoid* TFSI conformation is termed "TFSI-transoid"; and the simulation employing the *biased cisoid* TFSI conformation is termed "TFSI-cisoid". For each of these three simulations, RDFs between illustrative cation/anion atom pairs are shown in Figure 11; these RDFs depict the correlation between the nitrogen and oxygen atoms of TFSI and nitrogen and carbon atoms of the imidazolium ring (C_{ring}, N_{ring}) of BMIM.

Interestingly, there is a very prominent structural difference between the simulations, namely, the close-distance shoulder in the C_{ring}–N_{TFSI} and N_{ring}–N_{TFSI} RDFs that is present in the TFSI-flexible and TFSI-cisoid simulation but not in the TFSI-transoid simulation. This feature in the RDFs indicates that cisoid TFSI conformations are able to achieve closer contact with the BMIM cations compared to transoid conformations. In Figure 12, we show snapshots of BMIM/TFSI close-contact ion-pair interactions for both transoid and cisoid TFSI conformations (the selection of these particular configurations is discussed below). These representative configurations indicate that cisoid conformations of TFSI can achieve closer interaction with the imidazolium ring of BMIM by positioning both $-SO_2$ groups directly above the ring with the oxygen atoms pointing toward the cation. These close-contact interactions between cations and cisoid anions explain the energetic bias for cisoid TFSI conformers observed for both ion pairs and bulk ILs, evidenced by the distribution in Figure 10. Our predicted cation/anion RDFs are qualitatively similar to

DOI: 10.1021/acs.jpcb.8b01221
J. Phys. Chem. B 2018, 122, 4101−4114

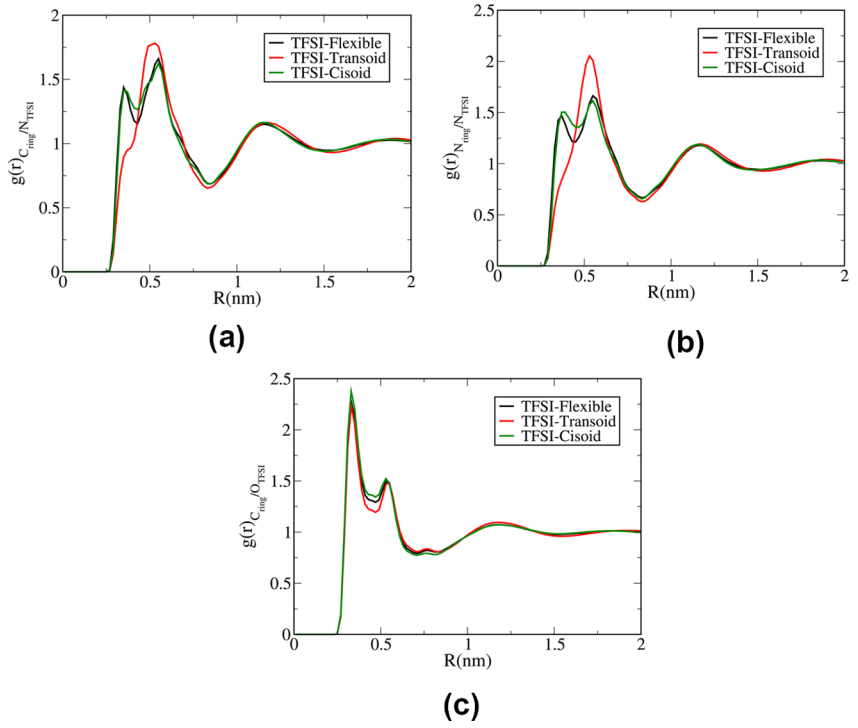

Figure 11. RDFs between atom pairs of cation and anion; (a) C_{ring} atoms of cation and N atoms of anion, (b) N_{ring} atoms of cation and N atoms of anion, and (c) C_{ring} atoms of cation and O atoms of anion. The notation "TFSI-flexible", "TFSI-transoid", and "TFSI-cisoid" denote the unbiased and biased MD simulations.

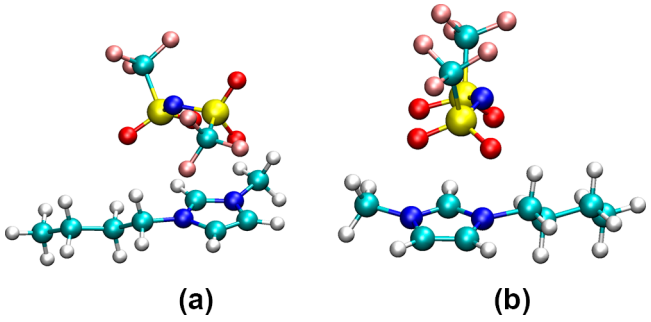

Figure 12. Representative local minima of [BMIM][TFSI] ion pairs for (a) transoid TFSI and (b) cisoid TFSI conformations.

analogous RDFs computed for the EMIM/TFSI IL from recent ab initio MD (AIMD) simulations.[68]

Other thermodynamic and transport properties are also strongly influenced by the TFSI conformations. The cohesive energy of [BMIM][TFSI] calculated from the TFSI-cisoid simulation is ∼6−8 kJ/mol more attractive (per ion pair) than that computed from the original simulation (Table 1). Interestingly, the TFSI-flexible simulation predicts the highest density, and the density is ∼1% lower in the TFSI-cisoid simulation, with an intermediate density for the TFSI-transoid simulation. This indicates that transoid TFSI conformers pack more efficiently than cisoid conformers in the bulk [BMIM][TFSI] IL, whereas a combination of cisoid and transoid conformations gives the most efficient packing. Thus, the fractional composition of cisoid and transoid TFSI conformers in the liquid is dictated by both energetics and ion packing, in contrast to gas-phase ion pairs in which conformations are dictated purely based on energetics (Figure 10). We speculate that the relatively inefficient packing of cisoid conformers is due to ion-pair interactions similar to that shown in Figure 12b, in which the $-CF_3$ groups are both oriented directly opposite of the cation/anion coordination vector, such that they form a "hydrophobic" buffer on one side of the TFSI anion.

To further explore the TFSI conformational influence on the cohesive energy density, we randomly select ∼300 BMIM/TFSI ion pairs from the bulk IL that are within the van der Waals contact separation. We then compute interaction energies for the cation/anion pairs, after minimizing the dimer geometries in the gas phase; this results in cation/anion local minima configurations that are representative of the bulk liquid. (The BMIM/TFSI close-contact configurations shown in Figure 12 are two representative local minima determined from this analysis.) The ion pairs with cisoid TFSI conformations exhibit an average of ∼15 kJ/mol greater attraction than ion pairs with transoid TFSI conformations, consistent with the cisoid-attributed close-contact shoulder in the RDFs (Figure 11). The difference in ion−ion interaction strength for the different TFSI conformations explains the fractional composition of [BMIM][TFSI] IL (Figure 10). While transoid TFSI has a lower conformational energy (Figure 2), the enhanced cation/anion attraction for cisoid TFSI conformations results in a greater fraction of these latter conformations in the bulk IL than predicted based on the conformational energy alone. This important influence of *inter*molecular interactions on the fractional conformational composition reflects the very large electrostatic interactions between ions and thus is a particularly important effect in ILs compared to neutral organic solvents. We speculate that the enhanced interaction of cisoid TFSI conformations with imidazolium cations may partially account for the cisoid TFSI conformations of DMIM/TFSI crystals.[17]

The anion dynamics depends sensitively on *interconversion* between the cisoid and transoid structures. For *both* the biased

DOI: 10.1021/acs.jpcb.8b01221
J. Phys. Chem. B 2018, 122, 4101−4114

TFSI-transoid and TFSI-cisoid simulations, we calculate anion diffusion coefficients that are ∼20−30% smaller than that predicted by the original, unbiased simulation. This indicates that interconversion between TFSI conformations is coupled to the translational ion dynamics, and the TFSI dihedral flexibility provides an important mechanism contributing to the structural relaxation of the bulk IL; we note similar findings by Borodin et al.[28] In Figure 13, we show a histogram of the interconversion

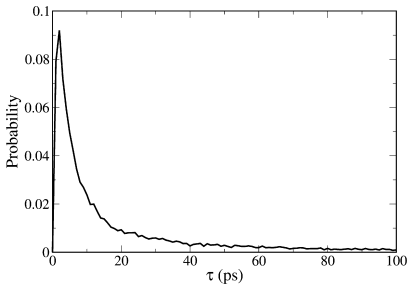

Figure 13. Histogram of interconversion times τ between transoid and cisoid TFSI conformations in [BMIM][TFSI] IL.

time (τ) between the transoid and cisoid TFSI conformations in the [BMIM][TFSI] IL (note this is computed using analogous classification scheme as in Figure 10). We find these interconversion times to be relatively short, on average generally several to tens of picoseconds, which is much faster than the diffusive regimes for translational motion; this confirms the importance of the anion flexibility for bulk transport. Additionally, the distribution in Figure 13 indicates that on ∼100 ps time scales, there is significant dynamic heterogeneity in [BMIM][TFSI] that is non-Gaussian. A significant fraction of TFSI anions exhibit much longer interconversion times than average, indicating local differences in the ion rearrangement within the bulk IL. We note that dynamic heterogeneity has been previously observed in other ILs,[69] and the coupling between structural and dynamic heterogeneity in TFSI-based ILs will be the subject of future investigation.

4. CONCLUSIONS

We have developed entirely ab initio force fields for organic anions TFSI, FSI, and OTf, and have described in detail our methodology for accurately parametrizing both conformational and intermolecular force field components. We have shown that small "probe" molecules can be employed to sample and fit the orientation dependence of short-range intermolecular interactions for the large organic anions. The resulting parametrization is robust, with exceptional transferability for describing the much larger-magnitude ion−ion interactions. We additionally have illustrated many subtle issues for accurately modeling the conformational flexibility of the organic anions. Because of coupling of equilibrium bonds and angles with torsion degrees of freedom, it is essential to consider both *relaxed* QM and *relaxed* MM PESs for modeling torsional flexibility with standard functional forms. Furthermore, constructing an appropriate MM Hamiltonian describing the conformational energetics is subtle and challenging because of the very large intramolecular electrostatic interactions of the point-charge model; such interactions can cause overpolarization of Drude oscillators and hinder an accurate representation of the conformational PES. Our specific resolution for TFSI, FSI, and OTf is to exclude the majority of intramolecular Coulombic interactions; however a general resolution for consistently describing intramolecular Coulombic interactions in MM models is an important challenge for future force field development.

The properties of [BMIM][TFSI], [BMIM][FSI], and [BMIM][OTf] ILs were predicted using MD simulations; as force field parameters were entirely determined based on ab initio calculations, this represents a truly first-principles prediction of the bulk liquid properties. Good agreement of predicted densities, heats of vaporization, ion diffusion coefficients, and conductivities was found with the available experimental data. While predicted IL densities were ∼2−3% too low, the IL density is extremely sensitive to ion packing and thus small changes in force field bond lengths (1−2%) result in significant density changes (3−5%). In contrast, the density is relatively insensitive to the liquid cohesive energy and thus is not an appropriate benchmark of nonbonded force field parameters. For [BMIM][TFSI], we predict that the bulk liquid consists of significant fractions of both cisoid and transoid TFSI conformations, which is largely influenced by the conformational dependence of the cation/anion interaction strength. Interconversion between these conformations occurs on several to tens of picosecond time scale, providing an important mechanism for structural relaxation that couples to translational ion diffusion rates.

We anticipate that future studies of TFSI-based electrolytes will establish complementary structure/property relationships involving the TFSI conformational flexibility. As the relative stability of cisoid and transoid conformers is dependent on intermolecular electrostatic interactions, both the fractional composition and interconversion rate will be modulated by the specific choice of cation for ILs.[14] Additionally, a recent study of mixing behavior in multicomponent ILs found that nonideal behavior was somewhat more common for TFSI-based IL mixtures, and it was suggested that the conformational flexibility was partially responsible.[70] As future electrolyte applications will involve a variety of mixture components,[13] interfaces,[71] and even nanoconfinement,[72] it will be important to characterize the conformational distribution of TFSI in these systems and the resulting influence on structure, energetics, and dynamics. In this respect, force fields that contain the correct balance of conformational and intermolecular energetics will be essential for accurately determining these physical processes.

■ ASSOCIATED CONTENT

Supporting Information

The Supporting Information is available free of charge on the ACS Publications website at DOI: 10.1021/acs.jpcb.8b01221.

Description of force field functional form; list of force field parameters developed in this work; comparisons of SAPT interaction energies to force field predictions for various ion-pair dimers; and torsional PES used for biased TFSI transoid and cisoid simulations (PDF)

Force field ".xml" files compatible with the OpenMM simulation software are additionally provided as supplementary material (ZIP)

■ AUTHOR INFORMATION

Corresponding Author

*E-mail: yethiraj@chem.wisc.edu.

DOI: 10.1021/acs.jpcb.8b01221
J. Phys. Chem. B 2018, 122, 4101−4114

ORCID

Jesse G. McDaniel: 0000-0002-9211-1108
Arun Yethiraj: 0000-0002-8579-449X

Present Address

[†]School of Chemistry and Biochemistry, Georgia Institute of Technology, Atlanta, Georgia 30332-0400 (J.G.M.).

Notes

The authors declare no competing financial interest.

■ ACKNOWLEDGMENTS

This research is supported by the Department of Energy, Basic Energy Sciences through grant DE-SC0017877. Computational resources were provided by the Center for High Throughput Computing at the University of Wisconsin. The CHTC is supported by UW-Madison, the Advanced Computing Initiative, the Wisconsin Alumni Research Foundation, the Wisconsin Institutes for Discovery, and the National Science Foundation and is an active member of the Open Science Grid, which is supported by the National Science Foundation and the U.S. Department of Energy's Office of Science. This research was supported in part by the National Science Foundation Grant CHE-0840494. Additional computational resources were provided through the Extreme Science and Engineering Discovery Environment (XSEDE) allocations under grant number TG-CHE090065.

■ REFERENCES

(1) Fedorov, M. V.; Kornyshev, A. A. Ionic Liquids at Electrified Interfaces. *Chem. Rev.* **2014**, *114*, 2978−3036.

(2) Armand, M.; Endres, F.; MacFarlane, D. R.; Ohno, H.; Scrosati, B. Ionic-liquid materials for the electrochemical challenges of the future. *Nat. Mater.* **2009**, *8*, 621−629.

(3) Zhang, S.; Sun, N.; He, X.; Lu, X.; Zhang, X. Physical Properties of Ionic Liquids: Database and Evaluation. *J. Phys. Chem. Ref. Data* **2006**, *35*, 1475−1517.

(4) Shkrob, I. A.; Marin, T. W.; Zhu, Y.; Abraham, D. P. Why Bis(fluorosulfonyl)imide Is a "Magic Anion" for Electrochemistry. *J. Phys. Chem. C* **2014**, *118*, 19661−19671.

(5) Dokko, K.; Tachikawa, N.; Yamauchi, K.; Tsuchiya, M.; Yamazaki, A.; Takashima, E.; Park, J.-W.; Ueno, K.; Seki, S.; Serizawa, N.; et al. Solvate Ionic Liquid Electrolyte for LiS Batteries. *J. Electrochem. Soc.* **2013**, *160*, A1304−A1310.

(6) Zhang, S. S. Liquid Electrolyte Lithium/Sulfur Battery: Fundamental Chemistry, Problems, and Solutions. *J. Power Sources* **2013**, *231*, 153−162.

(7) Suo, L.; Hu, Y.-S.; Li, H.; Armand, M.; Chen, L. A New Class of Solvent-in-Salt Electrolyte for High-Energy Rechargeable Metallic Lithium Batteries. *Nat. Commun.* **2013**, *4*, 1481.

(8) Xu, K. Electrolytes and Interphases in Li-Ion Batteries and Beyond. *Chem. Rev.* **2014**, *114*, 11503−11618.

(9) Fu, C.; Guo, J. Challenges and Current Development of Sulfur Cathode in LithiumSulfur Battery. *Curr. Opin. Chem. Eng.* **2016**, *13*, 53−62.

(10) Nowinski, J. L.; Lightfoot, P.; Bruce, P. G. Structure of $LiN(CF_3SO_2)_2$, a Novel Salt for Electrochemistry. *J. Mater. Chem.* **1994**, *4*, 1579−1580.

(11) Herstedt, M.; Smirnov, M.; Johansson, P.; Chami, M.; Grondin, J.; Servant, L.; Lassègues, J. C. Spectroscopic Characterization of the Conformational States of the Bis(trifluoromethanesulfonyl)imide Anion (TFSI). *J. Raman Spectrosc.* **2005**, *36*, 762−770.

(12) Fujii, K.; Fujimori, T.; Takamuku, T.; Kanzaki, R.; Umebayashi, Y.; Ishiguro, S.-i. Conformational Equilibrium of Bis-(trifluoromethanesulfonyl) Imide Anion of a Room-Temperature Ionic Liquid: Raman Spectroscopic Study and DFT Calculations. *J. Phys. Chem. B* **2006**, *110*, 8179−8183.

(13) Fujisawa, T.; Nishikawa, K.; Shirota, H. Comparison of interionic/intermolecular vibrational dynamics between ionic liquids and concentrated electrolyte solutions. *J. Chem. Phys.* **2009**, *131*, 244519.

(14) Vitucci, F. M.; Trequattrini, F.; Palumbo, O.; Brubach, J. B.; Roy, P.; Navarra, M. A.; Panero, S.; Paolone, A. Stabilization of Different Conformers of Bis(trifluoromethanesulfonyl)imide Anion in Ammonium-Based Ionic Liquids at Low Temperatures. *J. Phys. Chem. A* **2014**, *118*, 8758−8764.

(15) Shirota, H.; Kakinuma, S. Temperature Dependence of Low-Frequency Spectra in Molten Bis(trifluoromethylsulfonyl)amide Salts of Imidazolium Cations Studied by Femtosecond Raman-Induced Kerr Effect Spectroscopy. *J. Phys. Chem. B* **2015**, *119*, 9835−9846.

(16) Suarez, S. N.; Rúa, A.; Cuffari, D.; Pilar, K.; Hatcher, J. L.; Ramati, S.; Wishart, J. F. Do TFSA Anions Slither? Pressure Exposes the Role of TFSA Conformational Exchange in Self-Diffusion. *J. Phys. Chem. B* **2015**, *119*, 14756−14765.

(17) Holbrey, J. D.; Reichert, W. M.; Rogers, R. D. Crystal Structures of Imidazolium Bis(trifluoromethanesulfonyl)imide "ionic liquid" Salts: The First Organic Salt with a *cis*-TFSI Anion Conformation. *Dalton Trans.* **2005**, *15*, 2267.

(18) Maginn, E. J. Molecular Simulation of Ionic Liquids: Current Status and Future Opportunities. *J. Phys.: Condens. Matter* **2009**, *21*, 373101.

(19) Castner, E. W.; Wishart, J. F. Spotlight on ionic liquids. *J. Chem. Phys.* **2010**, *132*, 120901.

(20) Dommert, F.; Wendler, K.; Berger, R.; Delle Site, L.; Holm, C. Force Fields for Studying the Structure and Dynamics of Ionic Liquids: A Critical Review of Recent Developments. *ChemPhysChem* **2012**, *13*, 1625−1637.

(21) Salanne, M. Simulations of Room Temperature Ionic Liquids: from Polarizable to Coarse-Grained Force Fields. *Phys. Chem. Chem. Phys.* **2015**, *17*, 14270−14279.

(22) McDaniel, J. G.; Choi, E.; Son, C. Y.; Schmidt, J. R.; Yethiraj, A. Ab Initio Force Fields for Imidazolium-Based Ionic Liquids. *J. Phys. Chem. B* **2016**, *120*, 7024−7036.

(23) Uhlig, F.; Zeman, J.; Smiatek, J.; Holm, C. First-principles Parameterization of Polarizable Coarse-grained Force Fields for Ionic Liquids. *J. Chem. Theory Comput.* **2018**, *14*, 1471.

(24) Lopes, J. N. C.; Pádua, A. A. H. Molecular Force Field for Ionic Liquids Composed of Triflate or Bistriflylimide Anions. *J. Phys. Chem. B* **2004**, *108*, 16893−16898.

(25) Lopes, J. N. C.; Shimizu, K.; Pádua, A. A. H.; Umebayashi, Y.; Fukuda, S.; Fujii, K.; Ishiguro, S.-i. Potential Energy Landscape of Bis(fluorosulfonyl)amide. *J. Phys. Chem. B* **2008**, *112*, 9449−9455.

(26) Borodin, O.; Smith, G. D. Development of Many-Body Polarizable Force Fields for Li-Battery Applications: 2. LiTFSI-Doped Oligoether, Polyether, and Carbonate-Based Electrolytes. *J. Phys. Chem. B* **2006**, *110*, 6293−6299.

(27) Borodin, O.; Smith, G. D. Structure and Dynamics of N-Methyl-N-propylpyrrolidinium Bis(trifluoromethanesulfonyl)imide Ionic Liquid from Molecular Dynamics Simulations. *J. Phys. Chem. B* **2006**, *110*, 11481−11490.

(28) Borodin, O.; Gorecki, W.; Smith, G. D.; Armand, M. Molecular Dynamics Simulation and Pulsed-Field Gradient NMR Studies of Bis(fluorosulfonyl)imide (FSI) and Bis[(trifluoromethyl)sulfonyl]-imide (TFSI)-Based Ionic Liquids. *J. Phys. Chem. B* **2010**, *114*, 6786−6798.

(29) Zhao, W.; Eslami, H.; Cavalcanti, W. L.; Müller-Plathe, F. A Refined All-Atom Model for the Ionic Liquid 1-n-Butyl 3-Methylimidazolium bis(Trifluoromethylsulfonyl)imide [bmim]-[Tf2N]. *Z. Phys. Chem.* **2007**, *221*, 1647−1662.

(30) Logotheti, G.-E.; Ramos, J.; Economou, I. G. Molecular Modeling of Imidazolium-Based [Tf2N-] Ionic Liquids: Microscopic Structure, Thermodynamic and Dynamic Properties, and Segmental Dynamics. *J. Phys. Chem. B* **2009**, *113*, 7211−7224.

(31) Liu, H.; Maginn, E. A Molecular Dynamics Investigation of the Structural and Dynamic Properties of the Ionic Liquid 1-N-butyl-3-

DOI: 10.1021/acs.jpcb.8b01221
J. Phys. Chem. B 2018, 122, 4101−4114

methylimidazolium Bis(trifluoromethanesulfonyl)imide. *J. Chem. Phys.* **2011**, *135*, 124507.
(32) Zhong, X.; Liu, Z.; Cao, D. Improved Classical United-Atom Force Field for Imidazolium-Based Ionic Liquids: Tetrafluoroborate, Hexafluorophosphate, Methylsulfate, Trifluoromethylsulfonate, Acetate, Trifluoroacetate, and Bis(trifluoromethylsulfonyl)amide. *J. Phys. Chem. B* **2011**, *115*, 10027−10040.
(33) Borodin, O.; Smith, G. D. LiTFSI Structure and Transport in Ethylene Carbonate from Molecular Dynamics Simulations. *J. Phys. Chem. B* **2006**, *110*, 4971−4977.
(34) Borodin, O.; Smith, G. D. Structure and Dynamics of N-Methyl-N-propylpyrrolidinium Bis(trifluoromethanesulfonyl)imide Ionic Liquid from Molecular Dynamics Simulations. *J. Phys. Chem. B* **2006**, *110*, 11481−11490.
(35) Borodin, O. Polarizable Force Field Development and Molecular Dynamics Simulations of Ionic Liquids. *J. Phys. Chem. B* **2009**, *113*, 11463−11478.
(36) Bedrov, D.; Borodin, O.; Li, Z.; Smith, G. D. Influence of Polarization on Structural, Thermodynamic, and Dynamic Properties of Ionic Liquids Obtained from Molecular Dynamics Simulations. *J. Phys. Chem. B* **2010**, *114*, 4984−4997.
(37) McDaniel, J. G.; Schmidt, J. R. Physically-Motivated Force Fields from Symmetry-Adapted Perturbation Theory. *J. Phys. Chem. A* **2013**, *117*, 2053−2066.
(38) McDaniel, J. G.; Schmidt, J. R. Next-Generation Force Fields from Symmetry-Adapted Perturbation Theory. *Annu. Rev. Phys. Chem.* **2016**, *67*, 467−488.
(39) Jeziorski, B.; Moszynski, R.; Szalewicz, K. Perturbation-Theory Approach to Intermolecular Potential-Energy Surfaces of Van-Der-Waals Complexes. *Chem. Rev.* **1994**, *94*, 1887−1930.
(40) Szalewicz, K.; Patkowski, K.; Jeziorski, B. In *Intermolecular Forces and Clusters II*; Wales, D. J., Ed.; Structure and Bonding; Springer Berlin Heidelberg, 2005; Vol. *116*, pp 43−117.
(41) Szalewicz, K. Symmetry-adapted perturbation theory of intermolecular forces. *Wiley Interdiscip. Rev.: Comput. Mol. Sci.* **2012**, *2*, 254−272.
(42) Pronk, S.; Páll, S.; Schulz, R.; Larsson, P.; Bjelkmar, P.; Apostolov, R.; Shirts, M. R.; Smith, J. C.; Kasson, P. M.; van der Spoel, D.; et al. GROMACS 4.5: A High-Throughput and Highly Parallel Open Source Molecular Simulation Toolkit. *Bioinformatics* **2013**, *29*, 845−854.
(43) Plimpton, S. Fast Parallel Algorithms for Short-Range Molecular Dynamics. *J. Comput. Phys.* **1995**, *117*, 1−19.
(44) Eastman, P.; Friedrichs, M. S.; Chodera, J. D.; Radmer, R. J.; Bruns, C. M.; Ku, J. P.; Beauchamp, K. A.; Lane, T. J.; Wang, L.-P.; Shukla, D.; et al. OpenMM 4: A Reusable, Extensible, Hardware Independent Library for High Performance Molecular Simulation. *J. Chem. Theory Comput.* **2013**, *9*, 461−469.
(45) Heßelmann, A.; Jansen, G. Intermolecular Dispersion Energies from Time-Dependent Density Functional Theory. *Chem. Phys. Lett.* **2003**, *367*, 778−784.
(46) Heßelmann, A.; Jansen, G.; Schütz, M. Density-Functional Theory-Symmetry-Adapted Intermolecular Perturbation Theory with Density Fitting: A New Efficient Method to Study Intermolecular Interaction Energies. *J. Chem. Phys.* **2005**, *122*, 014103−014119.
(47) Misquitta, A. J.; Jeziorski, B.; Szalewicz, K. Dispersion Energy from Density-Functional Theory Description of Monomers. *Phys. Rev. Lett.* **2003**, *91*, 033201−033204.
(48) Misquitta, A. J.; Szalewicz, K. Symmetry-Adapted Perturbation-Theory Calculations of Intermolecular Forces Employing Density-Functional Description of Monomers. *J. Chem. Phys.* **2005**, *122*, 214109−214127.
(49) McDaniel, J. G.; Schmidt, J. R. First-Principles Many-Body Force Fields from the Gas Phase to Liquid: A "Universal" Approach. *J. Phys. Chem. B* **2014**, *118*, 8042−8053.
(50) Metz, M. P.; Piszczatowski, K.; Szalewicz, K. Automatic Generation of Intermolecular Potential Energy Surfaces. *J. Chem. Theory Comput.* **2016**, *12*, 5895−5919.
(51) Werner, H.-J.; Knowles, P. J.; Lindh, R.; Manby, F. R.; Schutz, M.; Celani, P.; Korona, T.; Mitrushenkov, A.; Rauhut, G.; Adler, T. B.; et al. MOLPRO, a Package of Ab Initio Programs, Version 2009.1. see http://www.molpro.net.
(52) Smith, J. C.; Karplus, M. Empirical force field study of geometries and conformational transitions of some organic molecules. *J. Am. Chem. Soc.* **1992**, *114*, 801−812.
(53) Jorgensen, W. L.; Maxwell, D. S.; Tirado-Rives, J. Development and Testing of the OPLS All-Atom Force Field on Conformational Energetics and Properties of Organic Liquids. *J. Am. Chem. Soc.* **1996**, *118*, 11225−11236.
(54) MacKerell, A. D.; Bashford, D.; Bellott, M.; Dunbrack, R. L.; Evanseck, J. D.; Field, M. J.; Fischer, S.; Gao, J.; Guo, H.; Ha, S.; et al. All-Atom Empirical Potential for Molecular Modeling and Dynamics Studies of Proteins. *J. Phys. Chem. B* **1998**, *102*, 3586−3616.
(55) Scott, W. R. P.; Hünenberger, P. H.; Tironi, I. G.; Mark, A. E.; Billeter, S. R.; Fennen, J.; Torda, A. E.; Huber, T.; Krüger, P.; van Gunsteren, W. F. The GROMOS Biomolecular Simulation Program Package. *J. Phys. Chem. A* **1999**, *103*, 3596−3607.
(56) Yu, H.; Whitfield, T. W.; Harder, E.; Lamoureux, G.; Vorobyov, I.; Anisimov, V. M.; MacKerell, A. D.; Roux, B. Simulating Monovalent and Divalent Ions in Aqueous Solution Using a Drude Polarizable Force Field. *J. Chem. Theory Comput.* **2010**, *6*, 774−786.
(57) Lamoureux, G.; Roux, B. Modeling Induced Polarization with Classical Drude Oscillators: Theory and Molecular Dynamics Simulation Algorithm. *J. Chem. Phys.* **2003**, *119*, 3025−3039.
(58) Basconi, J. E.; Shirts, M. R. Effects of Temperature Control Algorithms on Transport Properties and Kinetics in Molecular Dynamics Simulations. *J. Chem. Theory Comput.* **2013**, *9*, 2887−2899.
(59) Yeh, I.-C.; Hummer, G. System-Size Dependence of Diffusion Coefficients and Viscosities from Molecular Dynamics Simulations with Periodic Boundary Conditions. *J. Phys. Chem. B* **2004**, *108*, 15873−15879.
(60) Schröder, C. Collective Translational Motions and Cage Relaxations in Molecular Ionic Liquids. *J. Chem. Phys.* **2011**, *135*, 024502.
(61) Kashyap, H. K.; Annapureddy, H. V. R.; Raineri, F. O.; Margulis, C. J. How Is Charge Transport Different in Ionic Liquids and Electrolyte Solutions? *J. Phys. Chem. B* **2011**, *115*, 13212−13221.
(62) Lovelock, K. R. J. Quantifying Intermolecular Interactions of Ionic Liquids using Cohesive Energy Densities. *R. Soc. Open Sci.* **2017**, *4*, 171223.
(63) Tokuda, H.; Hayamizu, K.; Ishii, K.; Susan, M. A. B. H.; Watanabe, M. Physicochemical Properties and Structures of Room Temperature Ionic Liquids. 1. Variation of Anionic Species. *J. Phys. Chem. B* **2004**, *108*, 16593−16600.
(64) Tokuda, H.; Hayamizu, K.; Ishii, K.; Susan, M. A. B. H.; Watanabe, M. Physicochemical Properties and Structures of Room Temperature Ionic Liquids. 2. Variation of Alkyl Chain Length in Imidazolium Cation. *J. Phys. Chem. B* **2005**, *109*, 6103−6110.
(65) Verevkin, S. P.; Zaitsau, D. H.; Emel'yanenko, V. N.; Yermalayeu, A. V.; Schick, C.; Liu, H.; Maginn, E. J.; Bulut, S.; Krossing, I.; Kalb, R. Making Sense of Enthalpy of Vaporization Trends for Ionic Liquids: New Experimental and Simulation Data Show a Simple Linear Relationship and Help Reconcile Previous Data. *J. Phys. Chem. B* **2013**, *117*, 6473−6486.
(66) Nazet, A.; Sokolov, S.; Sonnleitner, T.; Makino, T.; Kanakubo, M.; Buchner, R. Densities, Viscosities, and Conductivities of the Imidazolium Ionic Liquids [Emim][Ac], [Emim][FAP], [Bmim]-[BETI], [Bmim][FSI], [Hmim][TFSI], and [Omim][TFSI]. *J. Chem. Eng. Data* **2015**, *60*, 2400−2411.
(67) Son, C. Y.; McDaniel, J. G.; Schmidt, J. R.; Cui, Q.; Yethiraj, A. First Principles United Atom Force Field for the Ionic Liquid [BMIM][BF4]: An Alternative to Charge Scaling. *J. Phys. Chem. B* **2016**, *120*, 3560−3568.
(68) Eilmes, A.; Kubisiak, P.; Brela, M. Explicit Solvent Modeling of IR and UVVis Spectra of 1-Ethyl-3-methylimidazolium Bis-(trifluoromethylsulfonyl)imide Ionic Liquid. *J. Phys. Chem. B* **2016**, *120*, 11026−11034.

DOI: 10.1021/acs.jpcb.8b01221
J. Phys. Chem. B 2018, 122, 4101−4114

(69) Zheng, Z.-P.; Fan, W.-H.; Roy, S.; Mazur, K.; Nazet, A.; Buchner, R.; Bonn, M.; Hunger, J. Ionic Liquids: Not only Structurally but also Dynamically Heterogeneous. *Angew. Chem., Int. Ed.* **2015**, *54*, 687−690.
(70) Clough, M. T.; Crick, C. R.; Gräsvik, J.; Hunt, P. A.; Niedermeyer, H.; Welton, T.; Whitaker, O. P. A Physicochemical Investigation of Ionic Liquid Mixtures. *Chem. Sci.* **2015**, *6*, 1101−1114.
(71) Liu, X.; Wang, Y.; Li, S.; Yan, T. Effects of Anion on the Electric Double Layer of Imidazolium-based Ionic Liquids on Graphite Electrode by Molecular Dynamics Simulation. *Electrochim. Acta* **2015**, *184*, 164−170.
(72) Bañuelos, J. L.; Feng, G.; Fulvio, P. F.; Li, S.; Rother, G.; Dai, S.; Cummings, P. T.; Wesolowski, D. J. Densification of Ionic Liquid Molecules within a Hierarchical Nanoporous Carbon Structure Revealed by Small-Angle Scattering and Molecular Dynamics Simulation. *Chem. Mater.* **2014**, *26*, 1144−1153.

DOI: 10.1021/acs.jpcb.8b01221
J. Phys. Chem. B 2018, 122, 4101−4114